

# Algorithms and Bounds for Distributed TDOA-Based Positioning Using OFDM Signals

Richard K. Martin, Chunpeng Yan, H. Howard Fan, *Senior Member, IEEE*, and Christopher Rondeau

**Abstract**—One main drawback of using time difference of arrival (TDOA) methods for source localization and navigation is that they require centralization of multiple copies of a signal. This paper considers blindly estimating the location of a cyclic prefix (CP) in an orthogonal frequency division multiplexing (OFDM) signal, enabling distributed TDOA computation up to an integer ambiguity. This ambiguity can be resolved using integer least-squares methods, if enough TDOAs are available, requiring only minimal cooperation between receivers. The contributions of this paper are development of an algorithm for simultaneously resolving the integer ambiguities and obtaining a position estimate; and derivation of the Cramér–Rao lower bound (CRLB) on locating the CP, and hence, on the underlying source localization and navigation problems.

**Index Terms**—Cramér–Rao lower bound (CRLB), orthogonal frequency division multiplexing (OFDM), source localization, time difference of arrival (TDOA), navigation.

## I. INTRODUCTION

POSITION awareness of mobile devices is becoming important in a variety of applications, including emergency response, law enforcement, military reconnaissance, location-based billing, resource allocation and tracking, and even handheld games. Two common positioning problems are source localization [1], [2], in which a network of nodes wishes to locate the source of a radio transmission, and navigation via signals of opportunity [3]–[5], [6], in which mobile users wish to determine their locations by exploiting commercial radio infrastructure. The latter problem arises in military contexts when the global positioning system (GPS) cannot be relied upon, or in commercial contexts when GPS signals are blocked by walls or terrain.

Manuscript received August 27, 2010; revised November 16, 2010; accepted November 24, 2010. Date of publication December 10, 2010; date of current version February 09, 2011. The associate editor coordinating the review of this manuscript and approving it for publication was Dr. Shengli Zhou. The work of R. Martin was supported in part by the Air Force Office of Scientific Research and by the Air Force Research Labs, Sensors Directorate. The views expressed in this paper are those of the authors, and do not reflect the official policy or position of the United States Air Force, Department of Defense, or the U.S. Government. This document has been approved for public release; distribution unlimited.

R. Martin and C. Rondeau are with the Department of Electrical and Computer Engineering, The Air Force Institute of Technology (AFIT), Wright-Patterson AFB, OH 45433-7765 USA (e-mail: richard.martin@afit.edu; christopher.rondeau@afit.edu).

C. Yan is with GIRD Systems, Inc., Cincinnati, OH 45221 USA (e-mail: cyan@girdsystems.com).

H. H. Fan is with the University of Cincinnati, Cincinnati, OH 45221 USA (e-mail: fan@ceecs.uc.edu).

Color versions of one or more of the figures in this paper are available online at <http://ieeexplore.ieee.org>.

Digital Object Identifier 10.1109/TSP.2010.2098404

Radio frequency (RF) based positioning is typically accomplished through some combination of angle of arrival (AOA) [1], received signal strength (RSS) [2], [7], time of arrival (TOA) [8], or time difference of arrival (TDOA) [9] measurements. AOA and RSS measurements are simple to obtain and use, but they require a dense network of receivers for high accuracy. TOA measurements require precise temporal synchronization and training between the transmitter and receiver [8]; thus, while they are quite accurate, they are not always practical. TDOA measurements are very accurate, but they typically require a bandwidth-intensive cross correlation between receivers [10], [11], [12]. Each of these methods has its distinct merits, but in this paper we focus on making TDOA measurements more practical.

The main drawback of using TDOA methods is that they require centralization (retransmitting each received signal to a central location) of multiple copies of a signal in order to perform cross-correlation. Centralization wastes bandwidth and power. For signals with a cyclic prefix (CP), such as orthogonal frequency division multiplexing (OFDM) or single-carrier cyclic-prefixed signals, the amount of centralization of data can be dramatically reduced by only comparing the temporal locations of the CPs rather than comparing the entire signals [13], [14]. To use the image registration parlance, this approach can be thought of as a “feature based” method, as opposed to “area based” methods such as cross correlation. CP detection can be done blindly, without *a priori* knowledge of the data contained in each CP [15], [16]. Thus, the TDOA computation can be distributed, and the data-sharing burden will be greatly reduced; but the final position estimation based on the TDOAs will still be centralized.

In this paper, we show how TDOA estimation and positioning can be performed for OFDM signals without any cross correlation of received signals. This involves locating the CPs within each received data stream, then resolving integer ambiguities in the TDOAs by exploiting the underlying positioning problem. Since CPs occur at regular intervals, finding a CP leaves an integer ambiguity in each TDOA—the actual TDOA may be the estimated TDOA plus any integer times the OFDM block length. This integer must be estimated, which is sometimes called integer ambiguity resolution. Previous work removed this ambiguity by cross-correlating a small amount of data [13], [14], whereas this paper leverages some mathematical similarities with integer ambiguity resolution in GPS research [17]–[19]. Thus, several aspects of this contribution are related to existing literature, but the formulation as a whole is new.

We also derive the Cramér–Rao lower bound (CRLB) on how accurately a CP can be located, and use this to derive the

CRLBs on source localization and navigation that use the CP rather than cross-correlation to estimate TDOA. The CRLB on estimating the time delay of the CP has not appeared in the literature before. Although much previous work discusses the CRLB of TDOA-based positioning, existing work assumes that the TDOAs are computed via cross-correlation, either between sensors [10], [11], [20] or with a known training signal (i.e., by TOA) [21], [22]. The former requires a large amount of bandwidth between nodes, and the latter requires training; whereas in this paper, the TDOA is estimated blindly and in a distributed fashion, by comparing the delays of the CPs (estimated as in [15] and [16]) in pairs of received signals. Moreover, previous work for the navigation problem assumed that one of the receiver positions was known, whereas our CRLB treats the positions of both receivers as unknown.

Although we do not attempt to mitigate the multipath, we do evaluate its deleterious effects on the CRLB. There exist means of mitigating multipath in TDOA-based localization, such as [23], [24], and such a method could be used in conjunction with our approach to improve performance. Several related papers have also considered the CRLB for multipath channels; in [24], the CRLB on positioning is derived as a function of erroneous TDOA measurements, in [25] a geometric view was used to show the benefits of node cooperation on positioning, and in [26] the TDOA on ranging in multipath, but the multipath was assumed to be known. However, none of these cases addressed a more efficient means of TDOA computation and the associated CRLB, which is one focus of this paper.

In summary, the contributions of this paper are i) a new TDOA-based positioning algorithm that completely removes the requirement of cross-correlation between receivers, and ii) derivation of CRLBs for the positioning problem, where the “observations” can be either the full received data streams or just their autocorrelations. Both the cases of multipath absent and present are considered.

The remainder of this paper is organized as follows. Section II defines the system model and notation. Section III derives the position estimation algorithm. Section IV derives the CRLB on estimating the temporal location of a CP in an OFDM signal. This in turn is used to derive CRLBs on source localization and navigation algorithms that are based on only using the block synchronization of OFDM signals, without cross-correlation. Section V provides simulation results, and Section VI concludes the paper.

## II. MODEL, NOTATION, AND ASSUMPTIONS

Section II-A discusses the two aspects to the system model: the geographical layout and the RF signal model. Then Section II-B discusses our assumptions.

### A. System Model and Notation

First, consider the geographical layout, as depicted in Figs. 1 and 2 for the two similar problems of “navigation via signals of opportunity” and “source localization,” respectively. In the navigation problem, there are  $K$  transmitters at known locations and two receivers at unknown locations. The  $k$ th TDOA corresponds to transmitter  $k$ , and is determined by the two receivers.

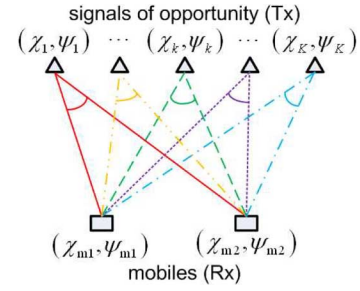


Fig. 1. Geographical layout for navigation via signals of opportunity. There are  $K$  transmitters at known locations and two receivers at unknown locations. The  $k$ th TDOA corresponds to transmitter  $k$ , and is determined by the two receivers.

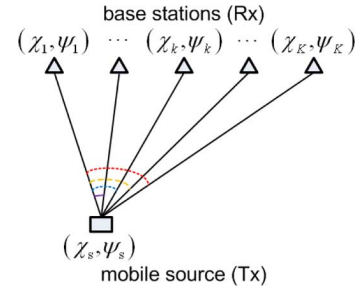


Fig. 2. Geographical layout for source localization. There are  $K$  receivers at known locations and one transmitter at an unknown location. The  $k$ th TDOA is determined by receiver  $k$  and receiver 1.

Throughout,  $\mathbf{x}$  denotes a two-dimensional position vector with Cartesian coordinates  $\chi$  and  $\psi$ . The transmitter locations are denoted  $\{\mathbf{x}_k = (\chi_k, \psi_k), k = 1, \dots, K\}$  and the mobiles are at locations  $\mathbf{x}_{m1} = (\chi_{m1}, \psi_{m1})$  and  $\mathbf{x}_{m2} = (\chi_{m2}, \psi_{m2})$ . There may also be a significant clock offset  $\tau$  between the two mobiles.

In contrast, source localization involves  $K$  receivers at known locations and one transmitter at an unknown location, and the  $K - 1$  TDOAs are jointly determined by the  $K$  receivers. The receiver locations are denoted  $\{\mathbf{x}_k = (\chi_k, \psi_k), k = 1, \dots, K\}$  and the source is at location  $\mathbf{x}_s = (\chi_s, \psi_s)$ . The receivers are assumed to coordinate to remove any clock offsets between them.

In the model for the RF signals, unless otherwise noted, we focus on a single transmitter and receiver and drop subscripts for clarity. We assume that the reader is somewhat familiar with OFDM and CPs. The OFDM transmitter uses a fast Fourier transform (FFT) size of  $N$ , a CP length of  $\nu$  samples, and a bandwidth of  $1/T$  Hz. The transmitter sends one block of  $M = N + \nu$  samples of  $x[k]$  every  $MT$  seconds. The set  $\mathcal{L}_c$  denotes the set of  $k$  in which  $x[k]$  is in a cyclic prefix (the first  $\nu$  of each  $M$  samples), the set  $\mathcal{I}_d$  denotes the indices of the unique  $N - \nu$  samples in the middle of each  $M$  samples, and the set  $\mathcal{L}_e$  denotes the indices of the last  $\nu$  of each  $M$  samples (which get copied into the CP).

The receiver uses an oversampling factor of  $q$ , and thus has a sampling period of  $T_s = T/q$ . The receiver samples a total of  $L$  blocks, or  $LqM$  samples. In the presence of multipath, with resolvable paths separated by  $T_s$  and a line-of-sight (LOS) path present, the received signal to be sampled is

$$y(t) = \sum_k x[k] \sum_{j=0}^J h[j] p(t - \delta_o T_s - kT - jT_s) + n(t) \quad (1)$$

TABLE I  
THE PRINCIPAL NOTATION USED IN THIS PAPER, FOR THE NAVIGATION (NAV)  
AND/OR SOURCE LOCALIZATION (SL) PROBLEMS. UNITS ARE IN BRACKETS,  
AND “RX” MEANS “RECEIVER”

|   |   |
|---|---|
| base station positions [m]                          | $\mathcal{X}_k = (\chi_k, \psi_k)$            |
| mobile positions (NAV) [m]                          | $\mathcal{X}_{m1}, \mathcal{X}_{m2}$          |
| mobile position (SL) [m]                            | $\mathcal{X}_s$                               |
| number of base stations                             | $K$   |
| baud period [s]                                     | $T$   |
| sampling period [s]                                 | $T_s$   |
| oversampling factor                                 | $q = T/T_s$                                   |
| FFT size [samples]                                  | $N$   |
| CP length [samples]                                 | $\nu$   |
| OFDM block length [samples]                         | $M = N + \nu$                                 |
| OFDM block length [m]                               | $\lambda = c TM$                              |
| number of OFDM blocks                               | $L$   |
| time indices $k$ in CP, data, end-of-block          | $\mathcal{I}_c, \mathcal{I}_d, \mathcal{I}_e$ |
| transmitted data (discrete time)                    | $x[k]$  |
| pulse shape (un-normalized, normalized)             | $p(t), p_o(t)$                                |
| multipath channel sampled at $T_s$                  | $h[j], j \in [0, J]$                          |
| received data                                       | $y(t)$  |
| delay (in [s], in [samples])                        | $\delta, \delta_o = \delta/T_s$               |
| distance from source to Rx $i$ (SL) [m]             | $r_{is}$                                      |
| distance from Rx $i$ to Rx $j$ (SL) [m]             | $r_{ij}$                                      |
| $c \times$ TDOA, Rx $i$ and $j$ (SL) [m]            | $d_{ij}^s = r_{is} - r_{js}$                  |
| $c \times$ estimated TDOA (SL) [m]                  | $\hat{d}_{ij}^s$                              |
| integer ambiguity for Rx $i$ and $j$ (SL)           | $z_{ij}$                                      |
| $c \times$ error in estimated $\delta$ , Tx $i$ [m] | $v_{is}$                                      |
| center of search space (SL) [m]                     | $\mathcal{X}_c = (\chi_c, \psi_c)$            |
| radius of search space (SL) [m]                     | $r_{\max}$                                    |

where  $x[k]$  is the transmitted data sequence (inverse FFT output and CP),  $p(t)$  is a raised-cosine pulse shape,  $\delta_o$  is the time delay to be estimated in units of samples,  $\delta = \delta_o T_s$  denotes the delay in seconds, and  $h[j]$  are the multipath coefficients. Like the transmitter, the noise  $n(t)$  is assumed to have a bandwidth of  $1/T$  Hz. The signal power and noise power are  $\sigma_x^2$  and  $\sigma_n^2$  per sample, respectively, and the signal-to-noise ratio (SNR) is  $\sigma_x^2/\sigma_n^2$ . The transmitted data is assumed to be white (aside from the presence of the CP), and the noise is assumed to be completely white over the spectrum of interest.

Note that *any* TDOA algorithm will suffer in the presence of multipath. The primary goal of this paper is not multipath mitigation, but rather analyzing and improving existing TDOA estimators. Once TDOAs are estimated, multipath mitigation can be incorporated into the positioning algorithm by discarding inconsistent TDOAs that are suspected to be corrupted due to multipath. That said, the CRLB and root mean squared error (RMSE) will be computed both in the absence of and in the presence of multipath.

We will use ticks to denote derivatives, e.g.,  $p'(t) = (d)/(dt)p(t)$ ; and subscripts “o” for normalization, e.g.,  $p(t) = p_o(t/T)$ . Throughout, the speed of light  $c$  will be used to convert temporal quantities into ranges as appropriate. The principal notation is summarized in Table I.

### B. Assumptions and Approximations

Throughout the paper, the base station positions are assumed to be known. In the source localization problem, the relative clock offsets between the base stations are assumed to be known; this could be accomplished by comparing TDOA estimates from a beacon transmitter at a known location (hence with known TDOAs). In the navigation problem, the clock

offset between receivers is unknown, and is estimated. It is assumed that there are no CFOs and that the transmitter parameters  $T$ ,  $N$ , and  $\nu$  are known.

The CRLB on time delay estimation is fundamentally concerned with continuous-time signals. However, provided that the transmitted signal and the noise are bandlimited, it is sufficient to assume that the received signal is sampled at the Nyquist rate [27, p. 54], i.e.,  $q = 1$ , which makes adjacent samples uncorrelated (although the proposed position estimation algorithm does allow for oversampling). The samples are still functions of continuous parameters (such as delay), so it is legitimate to differentiate the samples and functions thereof. Thus, all CRLB derivations are done in the context of baud-rate sampled data; however, the RMSE is evaluated both with and without oversampling.

We expect the RMSE to exhibit limiting effects at both high and low SNRs. At high SNRs, the performance of some estimators may be limited by the sampling period when the CRLB drops below the sample resolution. For example, the maximum likelihood (ML) algorithm of [15] does not interpolate between samples, hence its variance is at least that of a uniform random variable distributed over  $[-(1/2)T_s, (1/2)T_s]$ , which is  $(1)/(12)T_s^2$ . At low SNRs, the CRLB becomes arbitrarily large. However, since the search space for the CP location is a time window of  $MT$  seconds, the worst any estimator can do is to guess within this window with a uniform distribution, with a variance of  $(1)/(12)(MT)^2$  s<sup>2</sup>. This prior knowledge of the search space causes a bias to the estimator at low SNR, potentially allowing the RMSE to be below the (unbiased) CRLB. Thus, a standard deviation of  $cMT/\sqrt{12}$  m will be marked in the simulations as “upper bound,” and at low SNRs the RMSE will tend to this line rather than the CRLB.

## III. ESTIMATION ALGORITHMS

Position estimation is typically accomplished in two steps. First, the TDOAs are estimated from the RF data; and second, the position coordinates are estimated from the TDOAs. Section III-A reviews van de Beek’s synchronization algorithm for OFDM [15] and discusses how it can be used to partially accomplish TDOA estimation. Section III-B discusses how to combine these partial TDOA estimates with the position estimation problem to simultaneously resolve the remaining integer ambiguities in the TDOAs and produce position estimates. The novelty lies in a) formulating the OFDM TDOA problem in terms of integer ambiguity resolution, b) using a prior uncertainty region, the  $3\sigma$  bound on the noise, and the triangle inequality to restrict the search space as much as possible, and c) modifying integer ambiguity resolution and TDOA linearization algorithms from the GPS literature, and applying them to this problem. Each of these steps is not that challenging in and of itself, but no one has attempted anything like this for OFDM-based positioning so far as we know.

### A. TDOA Estimation

In [15], a ML algorithm was derived to jointly estimate the temporal location of the CP and the carrier frequency offset (CFO), but no CRLB was derived. In this paper, for simplicity, we assume there is no CFO. The ML algorithm of [15] assumed

no oversampling, i.e.,  $q = 1$ , hence it is not necessarily ML for  $q > 1$ . Accordingly, we will refer to it and its generalization as the van de Beek (vdB) algorithm. The vdB synchronization algorithm, generalized to allow for oversampling and averaging over  $L$  blocks, is given by

$$\hat{\delta}_{\text{vdB}} = \arg \max_{-\frac{Mq}{2} \leq \delta_o < \frac{Mq}{2}} \left\{ \gamma(\delta_o) - \frac{\rho}{2} \Phi(\delta_o) \right\} \quad (2)$$

$$\gamma(\delta_o) = \sum_{l=1}^L \sum_{k=Ml}^{Ml+\nu-1} y(kT + \delta_o T_s) y^* \times ((k+N)T + \delta_o T_s) \quad (3)$$

$$\Phi(\delta_o) = \sum_{l=1}^L \sum_{k=Ml}^{Ml+\nu-1} (|y(kT + \delta_o T_s)|^2 + |y((k+N)T + \delta_o T_s)|^2) \quad (4)$$

$$\rho = \frac{\text{SNR}}{\text{SNR} + 1}. \quad (5)$$

We will also consider a slight simplification of the vdB algorithm, given by

$$\hat{\delta}_{\text{acrr}} = \arg \max_{-\frac{Mq}{2} \leq \delta_o < \frac{Mq}{2}} \{ \gamma(\delta_o) \}. \quad (6)$$

The subscript ‘‘acrr’’ emphasizes the fact that this algorithm only uses the autocorrelation of the received signal, without the normalizing terms of the vdB algorithm. This is motivated by the fact that  $\Phi(\delta_o)$  is approximately constant over  $\delta_o$ , especially if the amount of averaging ( $L$ ) is large; and the  $\rho \Phi(\delta_o)$  term vanishes at low SNR.

Each receiver can synchronize to each transmission independent of the other transmitters and receivers. For the source localization problem (e.g.), two receivers  $i$  and  $j$  can estimate their TDOA by subtracting their synchronization estimates

$$\hat{d}_{ij}^{\text{ss}} = cT_s(\hat{\delta}_i - \hat{\delta}_j). \quad (7)$$

Since the underlying positioning problem requires working in distances, all TDOAs will be converted from time to range differences via a factor of  $c$ , as in (7), and the terms ‘‘TDOA’’ and ‘‘range difference’’ will be used interchangeably. (Note that range difference between two receivers is different from the distance between them, since range difference is with respect to a separate transmitter.) There will still be an integer ambiguity and measurement noise in the estimate

$$\hat{d}_{ij}^{\text{ss}} = \underbrace{(r_{is} - r_{js})}_{d_{ij}^{\text{ss}}} + \lambda z_{ij} + v_{is} - v_{js} \quad (8)$$

where  $r_{is}$  and  $r_{js}$  are the true distances between receivers  $i$ ,  $j$  and the source,  $\lambda = cTM$  is the length of an OFDM block converted to meters,  $z_{ij}$  is the unknown integer ambiguity, and  $v_{is}$  and  $v_{js}$  are the synchronization errors converted to distances. Without loss of generality,  $0 \leq \hat{d}_{ij}^{\text{ss}} < \lambda$ . Throughout,  $r$  will be used for a distance and  $d$  will be used for a range difference (i.e., a TDOA). The next section discusses how the underlying position estimation problem can be used to resolve the collection of integer ambiguities (one per TDOA).

## B. Position Estimation and Ambiguity Resolution

Here, we focus on source localization for clarity, but a similar discussion holds for the navigation problem. We also work in 2D rather than 3D for simplicity, but the approach generalizes easily. A TDOA estimate (8), expressed in distance rather than time, can be solved for the integer ambiguity as

$$z_{ij} = \frac{1}{\lambda} \left[ \hat{d}_{ij}^{\text{ss}} - (r_{is} - r_{js}) - (v_{is} - v_{js}) \right]. \quad (9)$$

With  $K$  receivers, there are  $K - 1$  TDOAs (all other TDOAs are linear combinations of these). However, there are  $K - 1$  integer ambiguities and two source coordinates, making  $K + 1$  unknowns. Thus the set of nonlinear location equations is under-determined. However, it can be easily shown that the unknown integers are bounded and there often exists a unique solution. The outline of our position estimation algorithm is as follows:

1. Difference the synchronization estimates from a pair of receivers to obtain a TDOA estimate with an integer ambiguity. Repeat for all possible TDOAs.
2. Use the triangle inequality and ‘‘3 $\sigma$  rule’’ to bound the unknown integers.
3. Partition the geographic search space into a number of smaller areas. Within each area, compute the integer bounds from step 2, temporarily assuming the source is within that area.
4. Linearize the TDOA equations and solve for the position and unknown integers, analogous to the methods used in [18], [28], [29], [30]. Repeat for each ‘‘small area’’ from Step 3.
5. Choose the ‘‘small area’’ that yields the solution whose estimated TDOAs from step 1 and predicted TDOAs (from the integer choices and position estimate in step 4) are most consistent.

There are two methods for bounding the unknown integers. The first is based on the triangle inequality and the 3 $\sigma$  rule (an unbounded Gaussian noise can be viewed as bounded by 3 $\sigma$ ), i.e.

$$|d_{ij}^{\text{ss}}| = |r_{is} - r_{js}| \leq r_{ij} \quad (10)$$

$$|v_{is} - v_{js}| \leq |v_{is}| + |v_{js}| \leq 6\sigma \quad (11)$$

where  $\sigma^2 = c^2 \text{VAR}[\hat{\delta}]$  is the variance of  $v_{is}$  and  $v_{js}$ , and  $r_{ij}$  is the known distance between receivers  $i$  and  $j$  (not to be confused with  $d_{ij}$ , the range difference between  $i$  and  $j$ ). If  $\sigma^2$  is unknown, it can be approximated from the CRLB given later in this paper. Then by (9), we derive the bound

$$\left\lceil \frac{\hat{d}_{ij}^{\text{ss}} - r_{ij} - 6\sigma}{\lambda} \right\rceil \leq z_{ij} \leq \left\lfloor \frac{\hat{d}_{ij}^{\text{ss}} + r_{ij} + 6\sigma}{\lambda} \right\rfloor \quad (12)$$

where  $\lceil \cdot \rceil$  and  $\lfloor \cdot \rfloor$  are the ceiling and floor operators, since  $z_{ij}$  is an integer.

The second bound on the unknown integers is based on an assumption that the source is located within a circular area which is centered at  $\chi_c = [\chi_c, \psi_c]^T$  with a radius  $r_{\text{max}}$

$$\|\chi_s - \chi_c\| \leq r_{\text{max}}. \quad (13)$$

In practice, we always have some kind of rough prior knowledge of the location of the source, since in terrestrial applications there is a limit on wireless communication ranges. Moreover, if our prior knowledge is very rough, a large area can be partitioned into many smaller areas, and for each smaller area, the constraint (13) can be applied. We assume this partitioning is required in the rest of this section and in the simulations. From (13), the triangle inequality bounds  $r_{is}$  and  $r_{js}$  by

$$l_{is} \triangleq \max(r_{ic} - r_{\max}, 0) < r_{is} < (r_{ic} + r_{\max}) \triangleq u_{is} \quad (14)$$

$$l_{js} \triangleq \max(r_{jc} - r_{\max}, 0) < r_{js} < (r_{jc} + r_{\max}) \triangleq u_{js} \quad (15)$$

where  $r_{ic} = \|\chi_i - \chi_c\|$ . Then from (8) and the  $3\sigma$  rule, the unknown integer is bounded by

$$\left\lceil \frac{\hat{d}_{ij}^s - u_{is} + l_{js} - 6\sigma}{\lambda} \right\rceil \leq z_{ij} \leq \left\lfloor \frac{\hat{d}_{ij}^s - l_{is} + u_{js} + 6\sigma}{\lambda} \right\rfloor. \quad (16)$$

Taking the intersection of the intervals in (12) and (16) yields the overall bound on each unknown integer.

The next step in position estimation is to linearize the non-linear TDOA location equations by Taylor expansion. We partition the large search space into smaller areas, and use the center of each small area in turn as  $\chi_c$ . Besides tightening the bounds on the unknown integers, another benefit of the partitioning is mitigation of the error caused by linearization. This linearization is given by

$$r_{is}(\chi_s) = r_{ic} + \frac{\chi_c - \chi_i}{r_{ic}}(\chi_s - \chi_c) + \frac{\psi_c - \psi_i}{r_{ic}}(\psi_s - \psi_c). \quad (17)$$

Substituting two instances of (17) into (8), stacking the  $K - 1$  TDOAs  $\{\hat{d}_{1i}^s, i = 2, \dots, K\}$  to obtain a matrix-vector formulation<sup>1</sup> and rearranging yields

$$\underbrace{\hat{\mathbf{d}} - \Delta \mathbf{r}_c + \mathbf{A} \chi_c}_{\mathbf{g}} = \mathbf{A} \chi_s + \mathbf{B} \mathbf{z} + \Delta \mathbf{v}$$

where  $\Delta \mathbf{r}_c$  is a vector with  $(i - 1)$ th element  $r_{1c} - r_{ic}$ ,  $\mathbf{z}$  is a vector containing the unknown integers  $z_{1i}$ ,  $\Delta v_{i-1} = v_{1s} - v_{is}$ ,  $\mathbf{B} = \lambda \mathbf{I}_{K-1}$ , and

$$\mathbf{A}_{(\text{row } i-1)} = \left[ \frac{\chi_c - \chi_1}{r_{1c}} - \frac{\chi_c - \chi_i}{r_{ic}}, \frac{\psi_c - \psi_1}{r_{1c}} - \frac{\psi_c - \psi_i}{r_{ic}} \right]. \quad (18)$$

$\mathbf{A} \in \mathcal{R}^{(K-1) \times 2}$  generally has full column rank, provided that we have a sufficient number of receivers and receivers are not clustered together. Assuming each  $v_{is}$  is Gaussian, the maximum likelihood estimates of  $\chi_s$  and  $\mathbf{z}$  must solve

$$\min_{\substack{\chi_s \in \mathcal{R}^2 \\ \mathbf{1} \leq \mathbf{z} \leq \mathbf{u}}} (\mathbf{g} - \mathbf{A} \chi_s - \mathbf{B} \mathbf{z})^T \mathbf{V}^{-1} (\mathbf{g} - \mathbf{A} \chi_s - \mathbf{B} \mathbf{z}) \quad (19)$$

where  $\mathbf{z}$  is constrained element-wise by bounds  $\mathbf{1}$  and  $\mathbf{u}$ , and  $\mathbf{V} = \sigma^2 [\mathbf{I} + \mathbf{1} \mathbf{1}^T]$  is the  $(K - 1) \times (K - 1)$  covariance matrix of  $\Delta \mathbf{v}$ . Here,  $\mathbf{1}$  is a  $(K - 1) \times 1$  vector of ones. This is a box-

constrained mixed integer least squares problem, since we have both the box-constrained integer unknowns  $\mathbf{z}$  and unconstrained real unknowns  $\chi_s$ .

We convert (19) to a standard form by using a Cholesky decomposition  $\mathbf{V} = \mathbf{R}^T \mathbf{R}$ . Then  $\bar{\mathbf{g}} = \mathbf{R}^{-T} \mathbf{g}$ ,  $\bar{\mathbf{A}} = \mathbf{R}^{-T} \mathbf{A}$ , and  $\bar{\mathbf{B}} = \mathbf{R}^{-T} \mathbf{B}$ .

$$\min_{\substack{\chi_s \in \mathcal{R}^2 \\ \mathbf{1} \leq \mathbf{z} \leq \mathbf{u}}} \|\bar{\mathbf{g}} - \bar{\mathbf{A}} \chi_s - \bar{\mathbf{B}} \mathbf{z}\|^2. \quad (20)$$

Let  $[\mathbf{Q}_A, \mathbf{R}_A]$  be the QR-decomposition of matrix  $\bar{\mathbf{A}}$ . Then let  $\bar{\mathbf{Q}}_A$  be obtained by deleting the first two columns of  $\mathbf{Q}_A$ . By ‘‘cancelling’’  $\chi_s$  as in [18], this equation can be converted to an underdetermined box-constrained integer least squares problem

$$\min_{\substack{\mathbf{z} \in \mathcal{R}^2 \\ \mathbf{1} \leq \mathbf{z} \leq \mathbf{u}}} \|\bar{\mathbf{g}} - \mathbf{H} \mathbf{z}\|^2 \quad (21)$$

where  $\mathbf{H} = \lambda^{-1} \bar{\mathbf{Q}}_A^H \bar{\mathbf{B}}$  is of dimension  $(K - 3) \times (K - 1)$  with full column rank, and  $\bar{\mathbf{g}} = \lambda^{-1} \bar{\mathbf{Q}}_A^H \bar{\mathbf{g}}$ .

Equation (21) is underdetermined with rank deficiency 2. The theory of this underdetermined box-constrained integer least squares problem has been developed for sphere decoding in multiple-input–multiple-output (MIMO) systems. With minor modification, the method of [28, Sec. 3] can be applied here to transform (21) to an overdetermined box-constrained integer least squares problem. Essentially, this method regularizes the problem by adding a penalty term to the cost function of the minimization problem. The penalty is proportional to the energy of the extra two variables in the solution’s search space.

Once the problem has been regularized, we apply the fast algorithm of [29] to solve the transformed (21). This involves two steps. First,  $\mathbf{H}$  is reduced to upper triangular form for efficiency of the search process [29, Sec. II.A]. Second, the DEC search algorithm of [29, Sec. II.B] is used to search through the constrained search space. Each element of  $\mathbf{z}$  is searched in turn until the best solution satisfying the constraints is found.

Applying a similar procedure to each small area, we obtain multiple integer solutions, i.e., a set of vectors  $\mathbf{z}$ . We substitute each of them back into (8) to get unambiguous range difference measurements, and use the linear method in [30] to calculate the estimated source location. At this point, we have a set of possible solutions (vector  $\mathbf{z}$  and the corresponding source location  $\chi_s$ ), one for each small area. We then select the one that makes the cost function (22) smallest as our final solution

$$\min (\hat{\mathbf{d}} - \mathbf{d}(\chi_s) - \lambda \mathbf{z})^T \mathbf{V}^{-1} (\hat{\mathbf{d}} - \mathbf{d}(\chi_s) - \lambda \mathbf{z}). \quad (22)$$

Essentially, we are checking for the best consistency (in the ML sense) between the estimated TDOAs  $\hat{\mathbf{d}}$  and the TDOA predicted by the  $\chi_s$  and  $\mathbf{z}$  from each region. This procedure will be validated in Section V.

The algorithm developed in this section has been for the source localization problem. In the analogous navigation problem, a similar algorithm could be developed. The steps in such an algorithm would parallel the five steps listed at the beginning of this subsection, but steps 3–5 would have to be generalized if the positions of more than one receiver are unknown.

<sup>1</sup>The TDOAs  $\hat{d}_{i-1,i}^s$  are another possible choice.

#### IV. CRLB DERIVATION

First, we derive the CRLB on estimating the delay of the CP given the entire observation record. Next, we consider the CRLB on estimators that only use the autocorrelation function of (3) to locate the CP. That is, we compute the bound on TDOA estimation for which *the autocorrelation function of (3) is considered to be the “observations,”* and otherwise the received data stream is not used. The resulting bound only applies to auto-correlation based estimators, e.g., (6); however, this includes most practical synchronization algorithms. This bound is derived both in the absence of and in the presence of multipath. Finally, we discuss how these bounds on the TDOA estimates affect the bounds on the position estimates, in both the navigation and positioning problems.

##### A. CRLB on Synchronization

As stated in Section II-B, in this section, there is no need for oversampling, i.e.,  $q = 1$ . The unknowns are the time delay  $\delta$  and the  $LN$  nuisance parameters in  $\mathbf{x}$ , consisting of the  $N$  unique samples of  $x[k]$  in each of the  $L$  blocks. The full CRLB calculation requires computing the matrix CRLB on the vector of all  $LN + 1$  parameters, and then examining the scalar bound on the parameter of interest. One possible alternate approach is to use the Modified CRLB (MCRLB) [31], in which the CRLB is evaluated as a function of the nuisance parameters, and then an expectation is computed over the nuisance parameters. Since the full CRLB is mathematically tractable here, we will not need to resort to the MCRLB. However, we will invoke ergodicity arguments to enable averaging over the nuisance parameters, in order to obtain bounds that are not dependant on  $\mathbf{x}$ .

The log-likelihood of the received vector  $\mathbf{y}$  is

$$\mathbf{y} = [y(T), \dots, y(LMT)]^T \quad (23)$$

$$\underbrace{\ln(f(\mathbf{y} | \mathbf{x}, \delta))}_{\mathcal{L}} = \text{const.} - \frac{1}{2\sigma_n^2} \sum_m [y(mT) - E\{y(mT)\}]^2 \quad (24)$$

$$E\{y(mT)\} = \sum_k x[k]p(mT - \delta - kT). \quad (25)$$

The Fisher information matrix (FIM) has a block structure

$$\mathbf{J} = \begin{bmatrix} \mathbf{A} & \mathbf{B}^T \\ \mathbf{B} & \mathbf{C} \end{bmatrix} \quad (26)$$

where  $\mathbf{A}$  is  $1 \times 1$ ,  $\mathbf{B}$  is  $LN \times 1$ , and  $\mathbf{C}$  is  $LN \times LN$ . In each dimension, the first element of  $\mathbf{J}$  corresponds to  $\delta$ , and then each successive set of  $N$  elements corresponds to a block of (unprefixed) independent data samples  $x[k]$ .

The (scalar) submatrix  $\mathbf{A}$ , evaluated at  $\delta = 0$  for simplicity, is

$$-E \left\{ \frac{\partial^2 \mathcal{L}}{\partial \delta^2} \right\} = \frac{1}{\sigma_n^2} \sum_m \left( \frac{\partial E\{y(mT)\}}{\partial \delta} \right)^2 \quad (27)$$

$$= \frac{1}{\sigma_n^2} \sum_m z^2[m] \quad (28)$$

$$z[m] \triangleq \sum_k x[k]p'((m - k)T). \quad (29)$$

Again for  $\delta = 0$ ,  $\mathbf{B}$  and  $\mathbf{C}$  are given element-wise by

$$-E \left\{ \frac{\partial^2 \mathcal{L}}{\partial \delta \partial x[k_0]} \right\} = \frac{1}{\sigma_n^2} \sum_m \frac{\partial E\{y(mT)\}}{\partial \delta} \frac{\partial E\{y(mT)\}}{\partial x[k_0]} \quad (30)$$

$$= \frac{-1}{\sigma_n^2} \sum_m z[m] \frac{\partial E\{y(mT_s)\}}{\partial x[k_0]} \quad (31)$$

$$-E \left\{ \frac{\partial^2 \mathcal{L}}{\partial x[k_0] \partial x[m_0]} \right\} = \frac{1}{\sigma_n^2} \sum_m \frac{\partial E\{y(mT)\}}{\partial x[k_0]} \frac{\partial E\{y(mT)\}}{\partial x[j_0]}. \quad (32)$$

Due to the repetition induced by the CP

$$\frac{\partial E\{y(mT)\}}{\partial x[k_0]} = \begin{cases} p((m - k_0)T), & k_0 \in \mathcal{I}_d \\ p((m - (k_0 - N))T) \\ + p((m - k_0)T), & k_0 \in \mathcal{I}_e. \end{cases} \quad (33)$$

For a Nyquist pulse shape, (33) becomes

$$\frac{\partial E\{y(mT)\}}{\partial x[k_0]} = \begin{cases} \delta_K(m, k_0), & k_0 \in \mathcal{I}_d \\ \delta_K(m, k_0 - N) + \delta_K(m, k_0), & k_0 \in \mathcal{I}_e \end{cases} \quad (34)$$

where  $\delta_K(\cdot)$  is the Kronecker delta function. Thus

$$\mathbf{A} = \frac{1}{\sigma_n^2} \sum_m z^2[m] \quad (35)$$

$$\mathbf{B}[k_0] = \frac{1}{\sigma_n^2} \cdot \begin{cases} -z[k_0], & k_0 \in \mathcal{I}_d \\ -z[k_0 - N] - z[k_0], & k_0 \in \mathcal{I}_e \end{cases} \quad (36)$$

$$\mathbf{C} = \frac{1}{\sigma_n^2} \begin{bmatrix} \mathbf{I}_{N-\nu} & \mathbf{0} \\ \mathbf{0} & 2\mathbf{I}_\nu \end{bmatrix} \otimes \mathbf{I}_L \quad (37)$$

where  $\otimes$  is the Kronecker product. (Note that  $k_0$  only indexes the last  $N$  of each  $N + \nu$  samples of  $x$ .) Using Schur complements to perform the matrix inversion in block fashion, the top left element of the CRLB is given by

$$\text{VAR}[\hat{\delta}] \geq [\mathbf{A} - \mathbf{B}^T \mathbf{C}^{-1} \mathbf{B}]^{-1} \quad (38)$$

$$= \sigma_n^2 \left[ \sum_m z^2[m] - \sum_{m \in \mathcal{I}_d} z^2[m] - \frac{1}{2} \sum_{m \in \mathcal{I}_e} (z[m] + z[m - N])^2 \right]^{-1} \quad (39)$$

In (39), there are three summations over the index  $m$ . The first summation includes all  $m$ , including the CP set,  $\mathcal{I}_c$ ; the data set,  $\mathcal{I}_d$ ; and the data in the ends of blocks,  $\mathcal{I}_e$ . The second summation only includes the data in the middle of each block, and the third summation only includes the data in the ends of blocks.

Breaking the sums from (39) into their constituent parts

$$\begin{aligned} \text{VAR}[\hat{\delta}] &\geq \sigma_n^2 \left\{ \sum_{j \in \mathcal{I}_c} z^2[j] + \sum_{j \in \mathcal{I}_d} z^2[j] + \sum_{j \in \mathcal{I}_e} z^2[j] - \sum_{j \in \mathcal{I}_d} z^2[j] \right. \\ &\quad \left. - \frac{1}{2} \sum_{j \in \mathcal{I}_e} (z^2[j] - 2z[j]z[j - N] + z^2[j - N]) \right\}^{-1}. \end{aligned}$$

Noting that “ $m \in \mathcal{I}_e$ ” is equivalent to “ $(m - N) \in \mathcal{I}_c$ .”

$$\begin{aligned} \text{VAR}[\hat{\delta}] &\geq 2\sigma_n^2 \left[ \sum_{m \in \mathcal{I}_e} (z[m] - z[m - N])^2 \right]^{-1} \\ &= 2\sigma_n^2 T^2 \left[ \sum_{m \in \mathcal{I}_e} \left( \sum_k (x[k] - x[k - N]) p'_o(m - k) \right)^2 \right]^{-1}. \end{aligned} \quad (40)$$

Observe that the terms when  $k \in \mathcal{I}_e$  are zero. Moreover, we always have  $m \in \mathcal{I}_e$ , and the pulse shape factor is nearly zero except when  $|m - k|$  is small. Thus, the terms that contribute most to the summation are the boundary terms, i.e., when  $k$  is just outside of  $\mathcal{I}_e$ .

Equation (41) is the CRLB, and cannot be simplified further without approximations. However, in order to gain intuition, consider the case of large  $L$ , which enables the approximation

$$\sum_{m \in \mathcal{I}_e} (\cdot) = L \cdot \frac{1}{L} \sum_{l=1}^L \sum_{m \in \mathcal{I}_e^l} (\cdot) \approx L \cdot \mathbb{E} \left\{ \sum_{m \in \mathcal{I}_e^l} (\cdot) \right\} \quad (42)$$

where the set  $\mathcal{I}_e^l$  is the data in block  $l$  of  $\mathcal{I}_e$ . Then, given that the data  $x[k]$  is uncorrelated (aside from the repetition in the CP),

$$\begin{aligned} \text{VAR}[\hat{\delta}] &\gtrsim 2\sigma_n^2 T^2 \left[ L \sum_{m \in \mathcal{I}_e^l} \sum_{k \notin \mathcal{I}_e} (2\sigma_x^2) (p'_o(m - k))^2 \right]^{-1} \\ &= \frac{T^2}{L \text{SNR}} \left[ \sum_{m \in \mathcal{I}_e^l} \sum_{k \notin \mathcal{I}_e} (p'_o(m - k))^2 \right]^{-1} \\ &= \frac{T^2}{L \text{SNR}} \left[ 2 \sum_{d=1}^{\infty} d (p'_o(d))^2 \right]^{-1} \end{aligned} \quad (43)$$

where the last line follows by tabulating all values of  $m$  and  $k$  allowed by the double summation and then counting occurrences of their difference  $d$ .

Since the TDOA is a subtraction of two delay estimates  $\hat{\delta}$ , its bound doubles relative to (43), hence

$$\boxed{\text{VAR}[\widehat{\text{TDOA}}_{\text{cp}}] \geq \frac{T^2}{L \text{SNR}} \underbrace{\left[ \sum_{d=1}^{\infty} d (p'_o(d))^2 \right]^{-1}}_{\eta}} \quad (44)$$

Equation (44) is the approximate CRLB, valid for values of  $L$  large enough to produce an averaging effect in (41). For raised cosine pulse shapes with excess bandwidths of 0, 0.25, and 0.5, the factor  $\eta$  is 0.63, 0.82, and 1.49, respectively.

For purposes of comparison, consider the CRLB on time-delay estimation using cross-correlation [10], [11] (as opposed to using the CP). Assume that  $L_{\text{xc}}$  samples are used for the cross-correlation (distinct from our parameter  $L$ , the number of CPs used in the autocorrelation). This bound is typically stated in terms of power spectra [10], [11], but an analogous bound has

been derived for signal shift estimation in the context of images [32], in an equivalent time domain (or spatial domain) form. With a little manipulation, the bound of [32] can be shown to be

$$\text{VAR}[\widehat{\text{TDOA}}_{\text{xc corr}}] \geq \frac{T^2}{L_{\text{xc}} \text{SNR}} \underbrace{\left[ \sum_{d=-\infty}^{\infty} (p'_o(d))^2 \right]^{-1}}_{\eta_{\text{xc}}}. \quad (45)$$

For raised cosine pulse shapes with excess bandwidths of 0, 0.25, and 0.5, the factor  $\eta_{\text{xc}}$  is 0.39, 0.48, and 0.78, respectively. The bound in (44) is quite similar to that of (45), save for the factor  $d$  in  $\eta$  and the dependence on  $L_{\text{xc}}$  rather than  $L$ . Since the factors  $\eta$  and  $\eta_{\text{xc}}$  are both on the order of unity, comparable values of the two bounds can be obtained by cross-correlating  $L_{\text{xc}}$  samples of two signals or by auto-correlating one signal using  $L$  OFDM blocks with  $L \approx L_{\text{xc}}$ , yielding a total duration of  $L_{\text{xc}} M$  samples. Thus, although our approach requires far less bandwidth use between the cooperative nodes, it requires a longer observation window to obtain a given accuracy.

### B. Bound for Autocorrelation-Based Methods

This section derives the CRLB for estimators that only use the autocorrelation data  $\gamma(t)$ , as in (6), without oversampling ( $q = 1$ ). Since in this subsection we assume that preprocessing of the data is performed to evaluate  $\gamma(t)$ , the values of  $\gamma(t)$  will be treated as observations, and the only unknown is the time delay  $\delta$ . This may seem contrary to the spirit of the CRLB, which is estimator-independent. However, the idea is that for a given set of observations, the bound is estimator-independent, yet in this section we restrict the observations. Thus, Section IV-A provided the bound for any algorithm that operates on the raw received data, and this section provides a higher bound for the subset of estimators that operate on the autocorrelation of the received data. It is higher since the preprocessed data provides less information than the raw data.

For later use, consider the following definitions, which are needed for Sections IV-B and -C only

$$\mu_{x,4} = \mathbb{E}\{|x|^4\} \quad (46)$$

$$h_2[n] = h[n] \star h^*[-n] \quad (47)$$

$$h_4[n] = h_2[n] \star h_2^*[-n] \quad (48)$$

$$\beta_1 = L \sigma_x^2 \quad (49)$$

$$\beta_2 = L (\mu_{x,4} h_4[0] - \sigma_x^4 h_4[0] + 2\sigma_x^2 \sigma_n^2 h_2[0] + \sigma_n^4) \quad (50)$$

$$\beta = \beta_1^2 / \beta_2 \quad (51)$$

$$\Lambda(t) = \begin{cases} \nu - |t/T|, & |t| \leq \nu T \\ 0, & \text{else.} \end{cases} \quad (52)$$

With a considerable amount of straightforward algebra (omitted here for conciseness), it can be shown that the second-order statistics of  $\gamma(t)$  are

$$\Gamma(t) \triangleq \mathbb{E}\{\gamma(t)\} = \beta_1 \Lambda(t - \delta) \star |h(t)|^2 \quad (53)$$

$$\text{COV}\{\gamma(t), \gamma(t + \tau)\} = \beta_2 \Lambda(\tau). \quad (54)$$

In the remainder of this subsection, we will ignore multipath (i.e.,  $h$  is an impulse), but we will return to it in the next subsection.

Let  $\boldsymbol{\gamma} = [\gamma(-M/2), \dots, \gamma(M/2 - 1)]$  be the vector of  $M$  samples of the autocorrelation function from (3), with mean vector  $\boldsymbol{\Gamma}$ . If  $L$  is large enough ( $L \gtrsim 10$  appears adequate), then by the Central Limit Theorem, samples of  $\boldsymbol{\gamma}$  have a Gaussian distribution, and the log-likelihood function of  $\boldsymbol{\gamma}$  given the delay  $\delta$  is

$$\underbrace{\ln(f(\boldsymbol{\gamma}|\delta))}_{\mathcal{L}} = \text{const.} - \frac{1}{2}(\boldsymbol{\gamma} - \boldsymbol{\Gamma})^T \mathbf{C}^{-1}(\boldsymbol{\gamma} - \boldsymbol{\Gamma}) \quad (55)$$

$$\mathbf{C}_{n_1, n_2} = \text{COV}\{\gamma(n_1 T), \gamma(n_2 T)\}. \quad (56)$$

Defining  $\mathbf{C}_o = \mathbf{C}/\beta_2$ , the Fisher information is given by

$$J = -\mathbb{E} \left\{ \frac{\partial^2 \mathcal{L}}{\partial \delta^2} \right\} = \frac{1}{\beta_2} (\boldsymbol{\Gamma}')^T \mathbf{C}_o^{-1} \boldsymbol{\Gamma}' \quad (57)$$

$$\mathbf{C}_{o, n_1, n_2} = \Lambda(n_2 T - n_1 T) \quad (58)$$

where  $\boldsymbol{\Gamma}'$  is a vector of samples of the time derivative of  $\Gamma(t)$ . Given the triangular shape of  $\Gamma(t)$ , its derivative has a *magnitude* of  $\beta_1/T$  for a range of  $2\nu$  samples, and is zero otherwise

$$\boldsymbol{\Gamma}' = (\beta_1/T) \cdot \mathbf{u}(\delta_o) \quad (59)$$

$$\mathbf{u}(\delta_o) = [\mathbf{0}_{1 \times (\delta_o - \nu)}, \mathbf{1}_{1 \times \nu}, -\mathbf{1}_{1 \times \nu}, \mathbf{0}_{1 \times (M - \delta_o - \nu)}]^T. \quad (60)$$

Factoring out constants and simplifying

$$J = \frac{(\beta_1/T)^2}{\beta_2} \underbrace{(\mathbf{u}(\delta_o))^T \mathbf{C}_o^{-1} \mathbf{u}(\delta_o)}_2 \quad (61)$$

where the value of  $\mathbf{u}^T \mathbf{C}_o^{-1} \mathbf{u} = 2$  has been evaluated numerically, and is constant regardless of the value of  $\delta$ . Simplifying

$$\text{VAR}[\hat{\delta}_{\text{corr}}] \geq \frac{\mu_{x,4} - \sigma_x^4 + 2\sigma_x^2 \sigma_n^2 + \sigma_n^4}{\sigma_x^4} \cdot \frac{T^2}{2L}. \quad (62)$$

However, for real and complex Gaussian time-domain signals,  $\mu_{x,4} = 3\sigma_x^4$  and  $2\sigma_x^4$ , respectively. Thus, for OFDM (typically complex Gaussian in the time-domain)

$$\text{VAR}[\hat{\delta}_{\text{corr}}] \geq \frac{(1 + \text{SNR}^{-1})^2 T^2}{2L}. \quad (63)$$

As in (44), the bound for the TDOA is doubled,

$$\boxed{\text{VAR}[\widehat{\text{TDOA}}_{\text{acorr}}] \geq \frac{(1 + \text{SNR}^{-1})^2 T^2}{L}}. \quad (64)$$

The limiting cases are

$$\text{VAR}[\widehat{\text{TDOA}}_{\text{acorr}}] \gtrsim \begin{cases} \frac{T^2}{L}, & \text{high SNR} \\ \frac{T^2}{L \text{SNR}^2}, & \text{low SNR.} \end{cases} \quad (65)$$

As expected, the bound of (64) is uniformly higher than the bound of (44), since only the autocorrelation of the received data is used in the estimator.

Interestingly (and counter-intuitively), both (44) and (64) are independent of the fraction of each block consisting of the CP, i.e., the fraction  $\nu/M$ . Thus, a short CP is as good as a long CP for purposes of blind delay estimation under the assumptions in this subsection (e.g., the absence of multipath). In Section V, this will be shown to be true for the RMSE of estimator performance as well.

The reason (65) levels off at high SNR is that the observations  $\gamma(t)$  are based on an auto-correlation of random signal data. Even in the absence of noise, the signal (and hence its autocorrelation) still has some variability, which can only be mitigated by averaging over more data (increasing  $L$ ).

### C. Effects of Multipath on Autocorrelation Methods

We now consider a multipath channel  $h(t)$ . In order to gain intuition, consider a simple multipath channel, with a LOS path of strength  $\sqrt{\alpha_0}$  and a single nonline-of-sight (NLOS) path of additional delay  $T$  and attenuation  $\sqrt{\alpha_1}$ . A complex phase could be added to each tap, but only the tap magnitudes squared affect the autocorrelation function  $\gamma(t)$ , hence the phases can be ignored. Then

$$h[n] = [\sqrt{\alpha_0}, \sqrt{\alpha_1}] \quad (66)$$

$$h_2[0] = \alpha_0 + \alpha_1, \quad (67)$$

$$h_4[0] = \alpha_0^2 + 4\alpha_0\alpha_1 + \alpha_1^2. \quad (68)$$

In order to not affect the received SNR, let  $\alpha_0 + \alpha_1 = 1$ .

Similar to the previous subsection, the log-likelihood function of  $\boldsymbol{\gamma}$  given the delay  $\delta$  and the nuisance parameters  $\alpha_0, \alpha_1$  is

$$\underbrace{\ln(f(\boldsymbol{\gamma}|\delta, \alpha_0, \alpha_1))}_{\mathcal{L}} = -\frac{1}{2}(\boldsymbol{\gamma} - \boldsymbol{\Gamma})^T \mathbf{C}^{-1}(\boldsymbol{\gamma} - \boldsymbol{\Gamma}). \quad (69)$$

From ([27, p. 47]), the FIM is given by

$$\mathbf{J}_{i,j} = \left( \frac{\partial \boldsymbol{\Gamma}}{\partial \theta_i} \right)^T \mathbf{C}^{-1} \frac{\partial \boldsymbol{\Gamma}}{\partial \theta_j} + \frac{1}{2} \text{tr} \left[ \mathbf{C}^{-1} \frac{\partial \mathbf{C}}{\partial \theta_i} \mathbf{C}^{-1} \frac{\partial \mathbf{C}}{\partial \theta_j} \right]. \quad (70)$$

The partial derivatives of the mean vector are

$$\boldsymbol{\Gamma}_\delta = (\beta_1/T) \cdot (\alpha_0 \mathbf{u}(\delta_o) + \alpha_1 \mathbf{u}(\delta_o + 1)) \quad (71)$$

$$\boldsymbol{\Gamma}_{\alpha_0} = \beta_1 \cdot \boldsymbol{\Lambda}(\delta_o) \quad (72)$$

$$\boldsymbol{\Gamma}_{\alpha_1} = \beta_1 \cdot \boldsymbol{\Lambda}(\delta_o + 1) \quad (73)$$

where  $\boldsymbol{\Lambda}(\delta_o)$  is a vector of samples of  $\Lambda(t)$ , with  $2\nu$  nonzero samples at the same locations as the nonzero samples of  $\mathbf{u}(\delta_o)$ . The channel (but not the delay) affects the scale factor  $\beta_2$ , but otherwise does not affect  $\mathbf{C}$ . Thus,

$$\mathbf{C}^{-1} \frac{\partial \mathbf{C}}{\partial \delta} = \mathbf{0} \quad (74)$$

$$\mathbf{C}^{-1} \frac{\partial \mathbf{C}}{\partial \alpha_i} = \frac{1}{\beta_2} \cdot \frac{\partial \beta_2}{\partial \alpha_i} \cdot \mathbf{I}_M \triangleq r_i \cdot \mathbf{I}_M \quad (75)$$

$$r_i \triangleq \frac{(\mu_{x,4} - \sigma_x^4)(2\alpha_i + 4\alpha_j) + 2\sigma_x^2 \sigma_n^2}{(\mu_{x,4} - \sigma_x^4) h_4[0] + 2\sigma_x^2 \sigma_n^2 h_2[0] + \sigma_n^4}. \quad (76)$$

The various products needed for the cross-terms of the first term of (70) can be shown to be

$$\mathbf{u}^T(\delta_o) \mathbf{C}_o^{-1} \mathbf{u}(\delta_o) = 2 \quad (77)$$

$$\mathbf{u}^T(\delta_o + 1) \mathbf{C}_o^{-1} \mathbf{u}(\delta_o) = 0 \quad (78)$$

$$\mathbf{u}^T(\delta_o) \mathbf{C}_o^{-1} \boldsymbol{\Lambda}(\delta_o) = 0 \quad (79)$$

$$\mathbf{u}^T(\delta_o + 1) \mathbf{C}_o^{-1} \boldsymbol{\Lambda}(\delta_o) = 1 \quad (80)$$

$$\mathbf{u}^T(\delta_o)\mathbf{C}_o^{-1}\mathbf{\Lambda}(\delta_o + 1) = -1 \quad (81)$$

$$\mathbf{\Lambda}^T(\delta_o)\mathbf{C}_o^{-1}\mathbf{\Lambda}(\delta_o) = \nu - 1/2 \quad (82)$$

$$\mathbf{\Lambda}^T(\delta_o)\mathbf{C}_o^{-1}\mathbf{\Lambda}(\delta_o + 1) = \nu \quad (83)$$

regardless of the value of  $\delta$ .

Putting all of this together, the  $3 \times 3$  FIM is given by

$$\mathbf{J} = \frac{\beta^2}{\beta_2} \begin{bmatrix} \frac{2}{T^2} (a_0^2 + a_1^2) & \frac{1}{T} a_1 & \frac{-1}{T} a_0 \\ \frac{1}{T} a_1 & \nu - \frac{1}{2} & \nu - 1 \\ \frac{-1}{T} a_0 & \nu - 1 & \nu - \frac{1}{2} \end{bmatrix} + \frac{M}{2} \begin{bmatrix} 0 & 0 & 0 \\ 0 & r_0^2 & r_0 r_1 \\ 0 & r_0 r_1 & r_1^2 \end{bmatrix}. \quad (84)$$

Using the cofactor method of obtaining elements of the inverse of a matrix, the (1, 1) element of the inverse of the FIM can be found, yielding

$$\text{VAR}[\hat{\delta}_{\text{corr}}] \geq \frac{T^2}{\beta} \frac{\beta + \frac{M}{2}(r_0 - r_1)^2}{(a_0 - a_1)^2 \beta + M(r_0 - r_1)^2 (a_0^2 + a_1^2)} \quad (85)$$

where comparatively smaller terms were dropped for compactness. The full numerically-determined value and this approximate value agree very well at low SNR and to within 10% at high SNR, for typical parameter values. The approximation is reported here in order to gain intuition. As in (44) and (64), the bound for the TDOA is doubled

$$\boxed{\begin{aligned} \text{VAR}[\widehat{\text{TDOA}}_{\text{multipath}}] \\ \geq \frac{T^2}{\beta} \frac{2\beta + M(r_0 - r_1)^2}{(a_0 - a_1)^2 \beta + M(r_0 - r_1)^2 (a_0^2 + a_1^2)} \end{aligned}} \quad (86)$$

where  $\beta = L(1 + \text{SNR}^{-1})^{-2}$ .

*Remarks:* First, if  $\alpha_i = 1$  and  $\alpha_{1-i} = 0$ , (86) almost reduces to (64), though (86) is slightly larger. In fact, for all possible parameter values, (86) is larger than (64). Second, if  $\alpha_0 = \alpha_1$ , then  $r_0 = r_1$ , and the bound becomes singular. This is because the function  $\Gamma(t)$  changes from a sharp peak to a flat-topped plateau. Thus, locally, the likelihood as a function of  $\delta$  is a constant. In practice, the variance of the delay estimator will not blow up, but the delay estimates will be evenly distributed across the delays of the two paths. The fact that the (finite) variance is below the (infinite) bound is due to estimator bias: in this case, the estimator is biased by half the temporal separation of the LOS path and the NLOS path, as depicted in Fig. 3.

Including more NLOS terms into the CRLB involves a straightforward generalization of (84). However, inverting the FIM could no longer be done in closed form, hence there would be little intuition to be gained. In Section V, we will evaluate the estimator variance and CRLB for various multipath profiles and strengths.

#### D. CRLB for Source Localization

Assume  $K$  synchronized TDOA receivers work together to locate one OFDM source. Given estimates of the CP delays  $\delta$  and a suitable method for resolving the integer ambiguities [18],

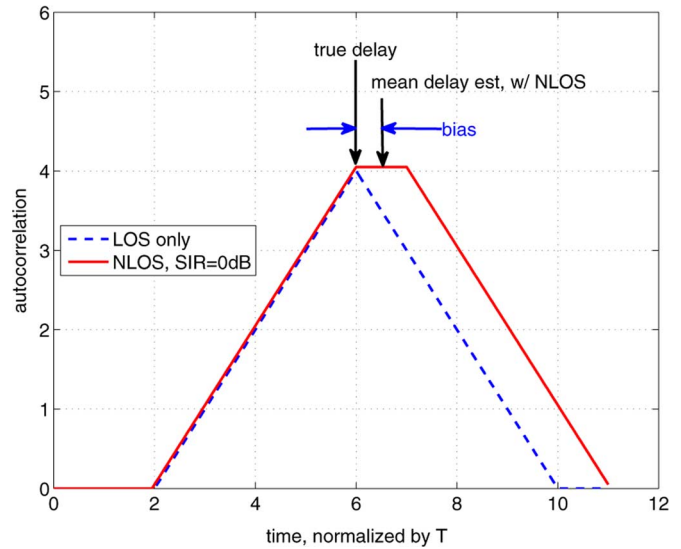


Fig. 3. Strong multipath can bias the delay estimator. This figure assumes  $\nu = 4$  and equal LOS and NLOS paths.

the TDOA between each pair of receivers can be obtained by subtracting two estimated delays  $\hat{\delta}$ . Thus, the vector of range difference estimates (converted from time to distance via  $c$ ) is

$$\hat{\mathbf{d}} = [\hat{d}_{12}, \hat{d}_{13}, \dots, \hat{d}_{1K}]^T \quad (87)$$

$$= c[\hat{\delta}_1 - \hat{\delta}_2, \hat{\delta}_1 - \hat{\delta}_3, \dots, \hat{\delta}_1 - \hat{\delta}_K]^T \quad (88)$$

with covariance matrix lower-bounded by  $\mathbf{Q}$ , where

$$\mathbf{Q} = \frac{(1 + \text{SNR}^{-1})^2 c^2 T^2}{2L} [\mathbf{I} + \mathbf{1}\mathbf{1}^T] \quad (89)$$

$$\mathbf{Q}^{-1} = \left( \frac{(1 + \text{SNR}^{-1})^2 c^2 T^2}{2L} \right)^{-1} \left[ \mathbf{I} - \frac{1}{K} \mathbf{1}\mathbf{1}^T \right] \quad (90)$$

where  $\mathbf{1}$  is a  $(K - 1) \times 1$  vector of ones. (If the SNRs differ per receiver, then the optimal Gauss-Markov TDOA estimator and its covariance matrix should be derived using (24)–(27) of [10].)

From (90) and the general form of the CRLB in [20], the CRLB on the position estimate can be computed given the covariance matrix of a TDOA estimator, as

$$\text{COV}[\mathbf{x}_s] \geq (\mathbf{G}^T \mathbf{Q}^{-1} \mathbf{G})^{-1} \quad (91)$$

$$= \frac{(1 + \text{SNR}^{-1})^2 c^2 T^2}{2L} \left( \mathbf{G}^T \left[ \mathbf{I} - \frac{1}{K} \mathbf{1}\mathbf{1}^T \right] \mathbf{G} \right)^{-1} \quad (92)$$

where  $\mathbf{G}$  is a  $(K - 1) \times 2$  matrix that depends entirely on the geometries of the transmitter and receivers, with the  $(i - 1)$ th row (for  $i = 2, 3, \dots, K$ ) given by

$$\mathbf{G}_{(\text{row } i-1)} = \left[ \frac{\chi_1 - \chi_s}{r_1} - \frac{\chi_i - \chi_s}{r_i}, \frac{\psi_1 - \psi_s}{r_1} - \frac{\psi_i - \psi_s}{r_i} \right] \quad (93)$$

where  $(\chi_s, \psi_s)$  and  $\{(\chi_i, \psi_i)\}$  are the locations of the source and  $K$  receivers, and  $r_i$  is the distance from the source to receiver  $i$ .

### E. CRLB for Navigation

Now consider the case in which  $K$  OFDM transmitters (signals of opportunity) are used by two receivers to perform navigation. The  $K$  transmissions are unrelated to each other, the transmitter positions  $\{(\chi_k, \psi_k), k = 1, \dots, K\}$  are known, the positions of both receivers are unknown, and the clock offset between the receiver clocks is unknown. Synchronization with the transmitter clocks is not required. Thus, there are 5 unknowns (or 7, in the 3D case): two coordinates for each receiver and one clock offset

$$\phi = [\chi_{m1}, \psi_{m1}, \chi_{m2}, \psi_{m2}, \tau]^T. \quad (94)$$

This section derives the CRLB for estimating these five parameters using  $K$  TDOAs, measured by the pair of receivers to each transmitter in turn.

Given the estimates of the CP locations and a suitable method for resolving the integer ambiguities, the range differences between each pair of receivers can be obtained by subtracting the two estimated delays

$$\hat{\mathbf{d}} = [\hat{d}_{12}^1, \hat{d}_{12}^2, \dots, \hat{d}_{12}^{sK}]^T \quad (95)$$

$$= c [\hat{\delta}_1^{s1} - \hat{\delta}_2^{s1}, \hat{\delta}_1^{s2} - \hat{\delta}_2^{s2}, \dots, \hat{\delta}_1^{sK} - \hat{\delta}_2^{sK}]^T. \quad (96)$$

The covariance matrix of  $\hat{\mathbf{d}}$  is lower-bounded by  $\mathbf{Q} = c^2 \sigma^2 \mathbf{I}_K$ , where  $\sigma^2$  is the right-hand side (RHS) of (64). Considering the clock offset between receivers, the  $K$  range difference estimates are distributed as

$$\hat{\mathbf{d}} \sim \mathcal{N}(\mathbf{d} + \tau c \mathbf{1}, c^2 \sigma^2 \mathbf{I}) \quad (97)$$

where  $\mathbf{d}$  is the true range difference vector, which depends on the unknown coordinates of the two receivers:

$$d_k = \sqrt{(\chi_k - \chi_{m1})^2 + (\psi_k - \psi_{m1})^2} - \sqrt{(\chi_k - \chi_{m2})^2 + (\psi_k - \psi_{m2})^2}. \quad (98)$$

For a Gaussian vector  $\hat{\mathbf{d}}$  as in (97), the CRLB is ([27, p. 47])

$$\mathbf{J}^{-1} = c^2 \sigma^2 \left( \frac{\partial(\mathbf{d} + \tau c \mathbf{1})^T}{\partial \phi} \frac{\partial(\mathbf{d} + \tau c \mathbf{1})}{\partial \phi} \right)^{-1}. \quad (99)$$

The partial derivatives are given by

$$\frac{\partial(\mathbf{d} + \tau c \mathbf{1})}{\partial \phi} = [\mathbf{G}_{m1}, -\mathbf{G}_{m2}, c \mathbf{1}] \quad (100)$$

where the form of each  $\mathbf{G}$  is somewhat different from that in the source localization problem (93) [20]

$$\mathbf{G}_{mi}^{(\text{row } k)} = \left[ \frac{-(\chi_k - \chi_{mi})}{\sqrt{(\chi_k - \chi_{mi})^2 + (\psi_k - \psi_{mi})^2}}, \frac{-(\psi_k - \psi_{mi})}{\sqrt{(\chi_k - \chi_{mi})^2 + (\psi_k - \psi_{mi})^2}}, c \right]$$

and, after inserting (64) for  $\sigma^2$ , the CRLB becomes

$$\mathbf{J}^{-1} = \frac{(1 + \text{SNR}^{-1})^2 c^2 T^2}{L} \times \begin{bmatrix} \mathbf{G}_{m1}^T \mathbf{G}_{m1} & -\mathbf{G}_{m1}^T \mathbf{G}_{m2} & c \mathbf{G}_{m1}^T \mathbf{1} \\ -\mathbf{G}_{m2}^T \mathbf{G}_{m1} & \mathbf{G}_{m2}^T \mathbf{G}_{m2} & -c \mathbf{G}_{m2}^T \mathbf{1} \\ c \mathbf{1}^T \mathbf{G}_{m1} & -c \mathbf{1}^T \mathbf{G}_{m2} & c^2 K \end{bmatrix}^{-1}. \quad (101)$$

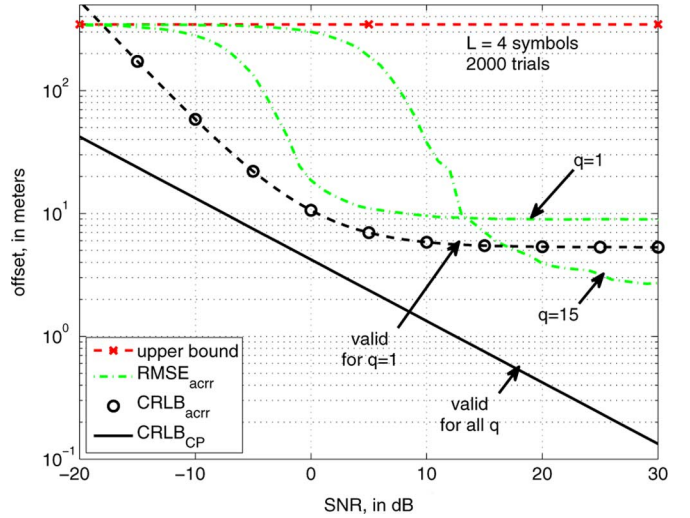


Fig. 4. The CRLB and the RMSE versus SNR, for  $\nu = 16$ ,  $N = 64$ , and  $L = 4$ . The estimators are given by (2) and (6). The upper bound corresponds to a uniform distribution across a span of  $MT$  s, as discussed in Section II-B.

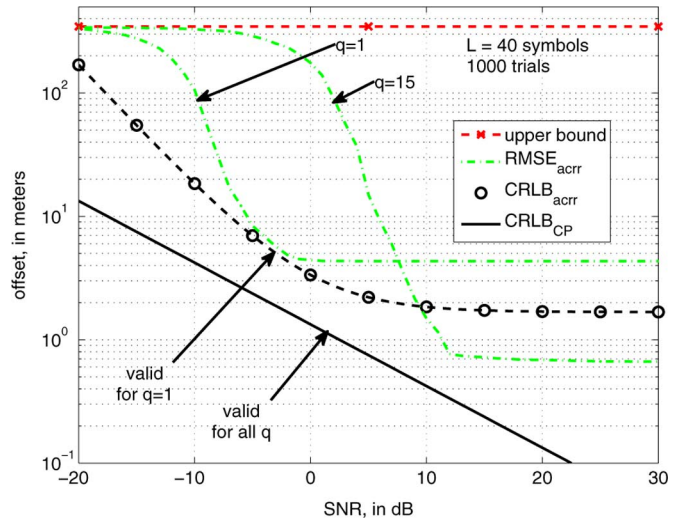


Fig. 5. The CRLB and the RMSE versus SNR, for  $\nu = 16$ ,  $N = 64$ , and  $L = 40$ . The estimators are given by (2) and (6).

The CRLB does not simplify further analytically, but it is simple to compute numerically. (It requires on the order of  $5^2 K + 5^3$  operations.)

## V. SIMULATIONS

The simulation parameters in this section are comparable to an IEEE 802.11a system: the FFT size is  $N = 64$ , the CP length is  $\nu = 16$ , the block size is  $M = N + \nu = 80$ , and the Nyquist sampling period is  $T = 50$  ns. Unless otherwise specified, the number of blocks is  $L = 10$  (yielding a 40  $\mu$ s observation window),  $q = 1$ , and the raised cosine pulse shape has no excess bandwidth.

The first set of results (Figs. 4 to 6) investigates the estimation of the CP delay. The RMSE of the vdB estimator of [15] and the simplified ‘‘acrr’’ estimator of (6) are compared to square root of the CRLBs from (44) and (64), using 2000 trials. The only difference between the figures is the number of blocks  $L$  used

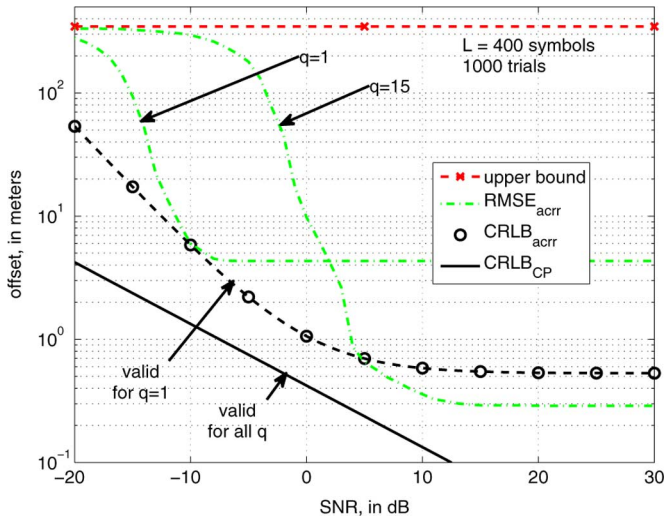


Fig. 6. The CRLB and the RMSE versus SNR, for  $\nu = 16$ ,  $N = 64$ , and  $L = 400$ . The estimators are given by (2) and (6).

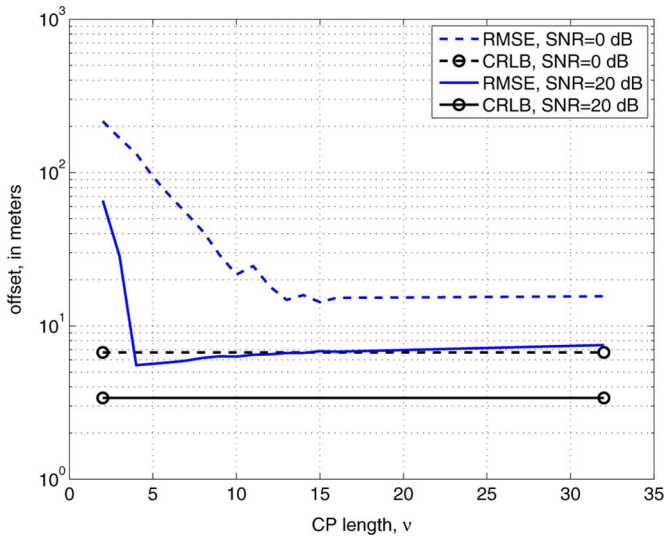


Fig. 7. Comparison of the CRLB and the RMSE of Van de Beek’s estimator versus the CP length  $\nu$ , for various values of SNR. Throughout,  $q = 1$ ,  $N = 64$ , and  $L = 10$ .

in averaging. These figures consider both  $q = 1$  and oversampling using  $q = 15$ . For all values of  $q$ , the RMSE must obey the general bound of (44); however, the “noise” signal in (54) is not bandlimited even though the noise in the raw signal  $y(t)$  is bandlimited. Thus, there is some benefit to oversampling when using autocorrelation-based methods. In principle, the bound of (64) could be generalized to account for oversampling; however, in that case, the correlation between subsampled data makes the derivation intractable. Thus, (54) is only applicable to the Nyquist-sampled case, whereas (44) applies regardless of oversampling.

Note that in Figs. 4 to 6, the RMSE tends to a “floor” based on the sampling resolution. That is, since the estimator does not attempt interpolation between samples, the resolution is limited by the variance within one sample period.

Fig. 7 compares the performance of the vdB estimator for various values of  $\nu$  to the CRLB. As indicated by (44) and (64),

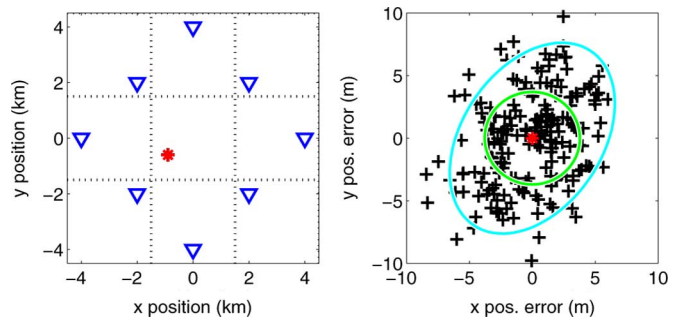


Fig. 8. Performance of position estimation, as in Section IV-D, for  $q = 1$ ,  $L = 10$ , and 10 dB SNR. Each  $\nabla$  is a sensor, the  $*$  is the source, and each  $+$  is a resolved source estimate (200 trials). The outer and inner ellipses indicate the RMSE and the CRLB, both scaled up by 2 so that the former gives an 86% confidence interval.

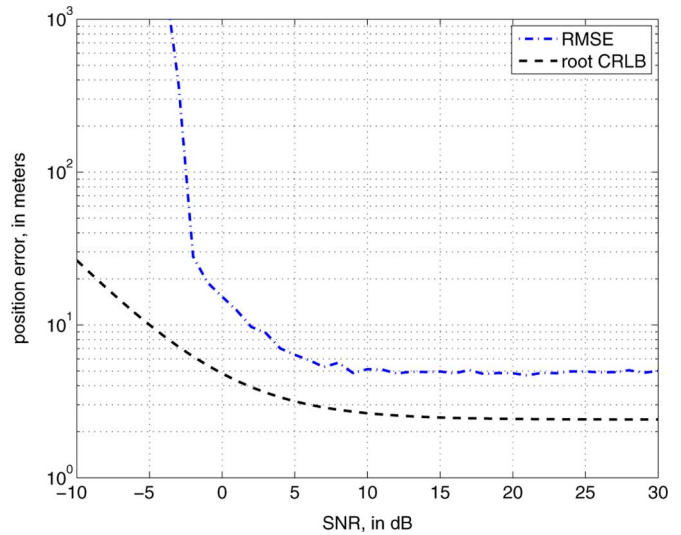


Fig. 9. Effects of varying SNR on position estimation error (in meters), for  $q = 1$ ,  $L = 10$ , and  $K = 8$  receivers.

the CRLB is not affected by the ratio  $\nu/M$ , i.e., the fraction of each block devoted to the CP. The RMSE also largely obeys this trend, although for shorter CP lengths, it is more sensitive to errors at low SNR.

The next set of results (Figs. 8 and 9) investigates the positioning step, once the CPs have already been located. Figs. 8 and 9 compare the final RMSE and the CRLB on position estimation, (92). Ambiguity resolution was performed by dividing the space into nine  $3 \text{ km} \times 3 \text{ km}$  regions, solving for the integer offsets within each region, and then choosing the region with the best solution as discussed in Section III-B. In Fig. 9, it can be inferred that the integer ambiguity resolution method breaks below about 0 dB SNR. Above that point, the position estimation standard deviation follows the CRLB; whereas below 0 dB SNR, the performance diverges sharply from the bound, as an increasing fraction of the integer estimates are wildly incorrect. The SNR location of this breakpoint tends to drop inversely proportionately to the square root of the value of  $L$  that is used (i.e., quadrupling  $L$  drops the breakpoint by 3 dB).

The final set of figures (Figs. 10 to 12) shows the effects of multipath, without any multipath mitigation attempted. Three

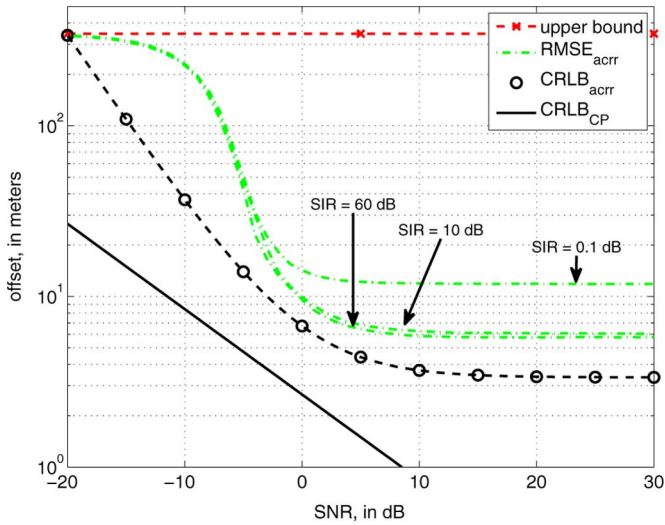


Fig. 10. Effects of multipath on RMSE. There are 1 LOS path and 1 NLOS path, and  $L = 10$ . The NLOS path is deterministic, but the curves for a Rayleigh-fading NLOS path are indistinguishable from these.

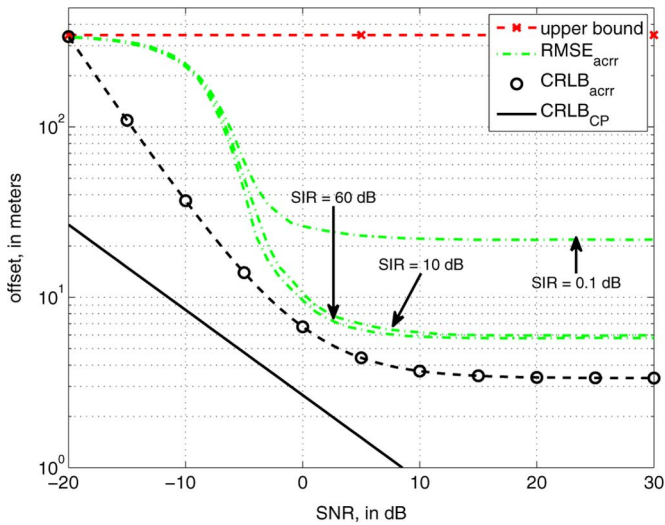


Fig. 11. Effects of multipath on RMSE. There are 1 LOS path and 5 Rayleigh-fading NLOS paths, and  $L = 10$ .

channels were considered: i) a LOS path with a single deterministic NLOS path, as in Section IV-C; ii) a LOS path with a single Rayleigh-fading NLOS path; and iii) a LOS path with five Rayleigh-fading NLOS paths. The signal-to-interference ratio (SIR) is the total power in the NLOS paths over the power of the LOS path. Fig. 10 shows the results for the single-NLOS case i), which are indistinguishable from those of case ii); and Fig. 11 shows the results for the many-NLOS case iii). Fig. 12 plots the results versus the SIR. As discussed in Section IV-C, at low SIR, the CRLB blows up; at the same time, the estimator becomes biased by the increasingly strong NLOS path. The RMSE of a biased estimator can be lower than the CRLB [27].

## VI. CONCLUSION

This paper considers blind, partially distributed positioning using OFDM signals, using TDOA measurements. The context

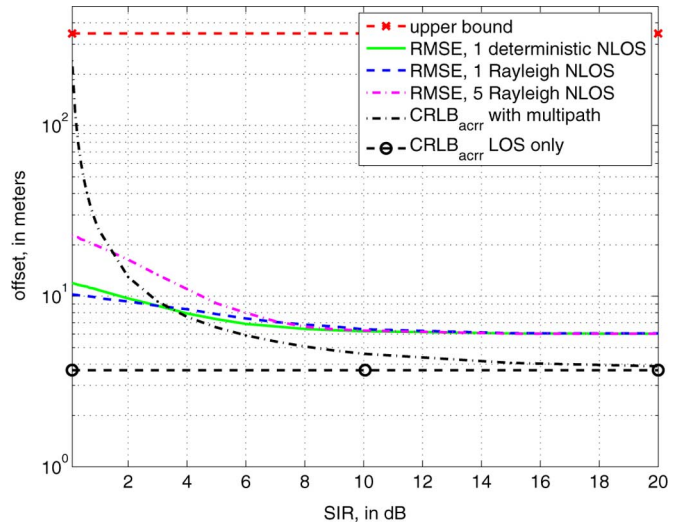


Fig. 12. Effects of multipath, at  $L = 10$  and an SNR of 10 dB. At low SNRs, the estimators are biased due to the NLOS path.

is either navigation via signals of opportunity or source localization. The method is partially distributed since all of the computation required for delay estimation is performed within each individual receiver by locating the temporal locations of the CPs. Then these time stamps are collected by a single node which jointly resolves the integer ambiguities (arising from the “which CP is which?” problem) and estimates the position of the mobile(s).

Under the assumption that the integer ambiguities can be resolved, the paper derived/discussed the following bounds:

- $\mathcal{B}1$ : (44) is the CRLB on estimating the TDOA by finding the CP in the received data.
- $\mathcal{B}2$ : (45) is the CRLB from the literature on estimating a TDOA via cross correlation.
- $\mathcal{B}3$ : (64) is the CRLB on estimating the TDOA by finding the CP using only autocorrelation data.
- $\mathcal{B}4$ : (86) generalizes  $\mathcal{B}3$  to include an unknown 2-ray multipath channel.
- $\mathcal{B}5$ : (92) uses  $\mathcal{B}3$  and the general CRLB of [20] to compute the CRLB on source localization.
- $\mathcal{B}6$ : (101) uses  $\mathcal{B}3$  and a method generalized from [20] to compute the CRLB on navigation.

A CRLB does not rely on the estimation method *per se*; however, it does rely on the data that is observed. In  $\mathcal{B}1$ , the observations are considered to be the raw received data, whereas in  $\mathcal{B}3$ , the observations are the empirically computed autocorrelation function of the observed data. These bounds do not state anything about the estimation method, though  $\mathcal{B}3$  does require preprocessing of the raw data to obtain the autocorrelation.  $\mathcal{B}1$  does not simplify to  $\mathcal{B}2$ , though they have parallels in structure. The novelty in  $\mathcal{B}1$  and  $\mathcal{B}3$  is not simply that the data is unknown, but that we are exploiting a modulation with a known structure (namely, the CP in OFDM).  $\mathcal{B}1$  and  $\mathcal{B}3$  do not apply to any arbitrary unknown waveform, and a generic bound that assumes an unknown but arbitrary waveform would not be useful

since it would not exploit the structure of OFDM. Simulation results were used to demonstrate that van de Beek's method of estimating of the CP location, coupled with our method of integer ambiguity resolution, performs close to the CRLB on positioning accuracy.

A portion of this paper (consisting of a preliminary version of parts of Sections IV and V) was presented at ICASSP 2009 [33].

## REFERENCES

- [1] G. Sun, J. Chen, W. Guo, and K. J. R. Liu, "Signal processing techniques in network-aided positioning," *IEEE Signal Process. Mag.*, vol. 22, pp. 12–23, Jul. 2005.
- [2] D. Blatt and A. O. Hero, III, "Energy-based sensor network source localization via projection onto convex sets," *IEEE Trans. Signal Process.*, vol. 54, no. 9, pp. 3614–3619, Sep. 2006.
- [3] T. D. Hall, "Radiolocation Using AM Broadcast Signals," Ph.D. dissertation, Mass. Inst. Technol., Cambridge, MA, Sep. 2002.
- [4] T. D. Hall, "Radiolocation using AM broadcast signals: The role of signal propagation irregularities," in *Proc. IEEE Position, Location and Navig. Symp. (PLANS)*, Monterey, CA, Apr. 2004, pp. 752–761.
- [5] K. A. Fisher, "The Navigation Potential of Signals of Opportunity-Based Time Difference of Arrival Measurements" Ph.D. dissertation, Air Force Inst. Technol., Wright-Patterson Air Force Base, OH, Mar. 2005 [Online]. Available: <http://handle.dtic.mil/100.2/ADA442340>
- [6] DARPA Strategic Technology Office, Robust Surface Navigation Program [Online]. Available: <http://www.darpa.mil/sto/space/rsn.html>
- [7] M. Rabbat and R. Nowak, "Decentralized source localization and tracking," in *Proc. Int. Conf. Acoust., Speech, Signal Process.*, Montreal, Canada, May 2004, vol. 3, pp. 921–924.
- [8] N. Patwari, J. N. Ash, S. Kyperountas, A. O. Hero, III, R. L. Moses, and N. S. Correal, "Locating the nodes: Cooperative localization in wireless sensor networks," *IEEE Signal Process. Mag.*, vol. 22, no. 4, pp. 54–69, Jul. 2005.
- [9] J. J. Caffery, Jr. and G. L. Stuber, "Overview of radiolocation in CDMA cellular systems," *IEEE Commun. Mag.*, vol. 36, no. 4, pp. 38–45, Apr. 1998.
- [10] W. R. Hahn and S. A. Tretter, "Optimum processing for delay-vector estimation in passive signal arrays," *IEEE Trans. Inf. Theory*, vol. 19, no. 9, pp. 608–614, Sep. 1973.
- [11] C. H. Knapp and G. C. Carter, "The generalized correlation method for estimation of time delay," *IEEE Trans. Acoust. Speech Signal Process.*, vol. 24, no. 4, pp. 320–327, Aug. 1976.
- [12] H. Wang and P. Chu, "Voice source localization for automatic camera pointing system in video conferencing," in *Proc. IEEE Int. Conf. Acoust, Speech, Signal Process.*, Munich, Germany, Apr. 1997, vol. 1, pp. 187–190.
- [13] R. K. Martin, J. S. Velotta, and J. F. Raquet, "Multicarrier modulation as a navigation signal of opportunity," in *Proc. IEEE Aerosp. Conf.*, Big Sky, MT, Mar. 2008.
- [14] R. K. Martin, J. Velotta, and J. Raquet, "Bandwidth efficient cooperative TDOA computation for multicarrier signals of opportunity," *IEEE Trans. Signal Process.*, vol. 57, no. 6, pp. 2311–2322, Jun. 2009.
- [15] J.-J. van de Beek, M. Sandell, and P. O. Borjesson, "ML estimation of time and frequency offset in OFDM systems," *IEEE Trans. Signal Process.*, vol. 45, no. 7, pp. 1800–1805, Jul. 1997.
- [16] J. Acharya, H. Viswanathan, and S. Venkatesan, "Timing acquisition for non contiguous OFDM based dynamic spectrum access," in *Proc. Dyn. Spectrum Access Netw. (DySpan)*, Chicago, IL, Oct. 2008.
- [17] P. J. G. Teunissen, "Least-squares estimation of the integer GPS ambiguities," in *Theory and Methodol.*, IAG General Meet., Beijing, China, Aug. 1993, vol. Sect. IV.
- [18] A. Hassibi and S. Boyd, "Integer parameter estimation in linear models with applications to GPS," *IEEE Trans. Signal Process.*, vol. 46, pp. 2938–2952, Nov. 1998.
- [19] T. D. Hall, C. C. Counselman, III, and P. Misra, "Instantaneous radiolocation using AM broadcast signals," in *Proc. 2001 Nat. Tech. Meet. Inst. Navigat.*, Long Beach, CA, Jan. 2001, pp. 93–99.
- [20] Y. T. Chan and K. C. Ho, "A simple and efficient estimator for hyperbolic location," *IEEE Trans. Signal Process.*, vol. 42, no. 8, pp. 1905–1915, Aug. 1994.
- [21] H. Reddy *et al.*, "An improved time-of-arrival estimation for WLAN-based local positioning," in *Proc. 2nd Int. Conf. on Commun. Syst. Software Middleware*, Jan. 2007.
- [22] C. Mensing, S. Plass, and A. Dammann, "Synchronization algorithms for positioning with OFDM communications signals," in *Proc. 4th Workshop on Positioning, Navigat. Commun.*, Mar. 2007, pp. 205–210.
- [23] J. Riba and A. Urruela, "A nonlinear-of-sight mitigation technique based on ML-detection," in *Proc. Int. Conf. Acoust., Speech Signal Process.*, May 2004, pp. 153–156.
- [24] Y. Qi, H. Kobayashi, and H. Suda, "Analysis of wireless geolocation in a nonlinear-of-sight environment," *IEEE Trans. Wireless Commun.*, vol. 5, no. 3, Mar. 2006.
- [25] M. Z. Win, Y. Shen, and H. Wymeersch, "On the position error bound in cooperative networks: A geometric approach," in *Proc. IEEE Int. Symp. Spread Spectrum Technol. Appl.*, Bologna, Italy, Aug. 2008.
- [26] R. Cardinali, L. De Nardis, P. Lombardo, and M.-G. Di Benedetto, "UWB ranging accuracy in high and low data rate applications," *IEEE Trans. Microw. Theory Techn.*, vol. 54, no. 4, pp. 1865–1875, Jun. 2006.
- [27] S. M. Kay, *Fundamentals of Statistical Signal Processing: Estimation Theory*. Englewood Cliffs, NJ: Prentice-Hall, 1993.
- [28] X.-W. Chang and X. Yang, "An efficient regularization approach for underdetermined MIMO system decoding," in *Proc. 2007 Int. Conf. Wireless Commun. Mobile Comput.*, Honolulu, HI, Oct. 2007, pp. 349–353.
- [29] X.-W. Chang and Q. Han, "Solving box-constrained integer least squares problems," *IEEE Trans. Wireless Commun.*, vol. 7, no. 1, pp. 277–287, Jan. 2008.
- [30] B. Friedlander, "A passive localization algorithm and its accuracy analysis," *IEEE Trans. Ocean. Eng.*, vol. 12, pp. 234–245, Jan. 1987.
- [31] R. W. Miller and C. B. Chang, "A modified Cramér–Rao bound and its applications," *IEEE Trans. Inf. Theory*, vol. 24, no. 3, pp. 398–400, May 1978.
- [32] D. Robinson and P. Milanfar, "Statistical performance analysis of super-resolution," *IEEE Trans. Image Process.*, vol. 15, no. 6, pp. 1413–1428, Jun. 2006.
- [33] R. K. Martin, C. Yan, and H. H. Fan, "Bounds on decentralized TDOA-based localization of OFDM sources," in *Proc. Int. Conf. Acoust., Speech, Signal Process.*, Taipei, Taiwan, Apr. 2009.

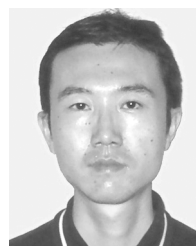


**Richard K. Martin** received dual B.S. degrees (*summa cum laude*) in physics and electrical engineering from the University of Maryland, College Park, in 1999, and the M.S. and Ph.D. degrees in electrical engineering from Cornell University, Ithaca, NY, in 2001 and 2004, respectively.

Since August 2004, he has been with the Department of Electrical and Computer Engineering, Air Force Institute of Technology (AFIT), Dayton, OH, where he is an Associate Professor. He is the author of 22 journal papers and 41 conference papers, and he

holds four patents. His research interests include navigation and source localization; cognitive radio; equalization for cyclic-prefixed systems; adaptive filters; sparse filters; and laser radar.

Dr. Martin has been elected Electrical and Computer Engineering Instructor of the Quarter three times and HKN Instructor of the Year twice by the AFIT students.



**Chunpeng Yan** received both the B.S. and M.S. degrees in electrical engineering from Shanghai Jiao Tong University (SJTU), Shanghai, China, in 1996 and 1999, respectively, and the Ph.D. degree in electrical engineering from the University of Cincinnati, Cincinnati, OH, in 2009.

Since 2008, he has been with Gird Systems, Inc. and has been working on GPS, wireless MIMO communication, and adaptive array related projects. His research interests are in the fields of adaptive and array signal processing, navigation, and digital

and wireless communications.



**H. Howard Fan** (SM'90) received the B.S. degree from Guizhou University, Guiyang, China, in 1976 and the M.S. and Ph.D. degrees from the University of Illinois, Urbana, in 1982 and 1985, respectively, all in electrical engineering.

From 1977 to 1978, he worked as a Research Engineer with the Provincial Standard Laboratory and Bureau of Guizhou Province, Guiyang. In 1978, he entered the Graduate School of the University of Science and Technology of China and then transferred to the University of Illinois, where he was a Teaching

and Research Assistant from 1982 to 1985. He joined the Department of Electrical and Computer Engineering, University of Cincinnati (UC), Cincinnati, OH, in 1985 as an Assistant Professor and is now a Professor. His research interests are in the general fields of systems and signal representation and reconstruction, system identification, adaptive signal processing, array signal processing, signal processing for communications, and location and navigation. He was a visiting researcher with the Systems and Control Group, Uppsala University, Uppsala, Sweden, in 1994. He was also a visiting researcher with the Air Force Research Lab., Dayton, OH, during 2008–2009.

Dr. Fan received the first ECE Departmental Distinguished Progress in Teaching Excellence Award from the UC in 1987, and was named Professor of the Quarter by UC College of Engineering and Engineering Tribunal for Winter Quarter 2005. He served as an Associate Editor of the IEEE TRANSACTIONS ON SIGNAL PROCESSING from 1991 to 1994. He is a member of Tau Beta Pi and Phi Kappa Phi.



**Christopher Rondeau** received the Masters degree from the Air Force Institute of Technology (AFIT), Dayton, OH, in December 2010.

He then reported to the U.S. Air Force Test Pilot School at Edwards Air Force Base, CA. He has held both sustainment engineering and test and evaluation positions during his Air Force assignments.